

## Local Measurement of the Eliashberg Function of Pb Islands: Enhancement of Electron-Phonon Coupling by Quantum Well States

Michael Schackert,<sup>1</sup> Tobias Märkl,<sup>1</sup> Jasmin Jandke,<sup>1</sup> Martin Hölzer,<sup>2</sup> Sergey Ostanin,<sup>2</sup> Eberhard K. U. Gross,<sup>2</sup> Arthur Ernst,<sup>2,3</sup> and Wulf Wulfhekel<sup>1</sup>

<sup>1</sup>Physikalisches Institut, Karlsruhe Institute of Technology, Wolfgang-Gaede-Straße 1, 76131 Karlsruhe, Germany

<sup>2</sup>Max-Planck Institut für Mikrostrukturphysik, Weinberg 2, 06120 Halle, Germany

<sup>3</sup>Wilhelm-Ostwald-Institut für Physikalische und Theoretische Chemie, Universität Leipzig, Linnéstraße 2, 04103 Leipzig, Germany

(Received 5 February 2014; revised manuscript received 30 May 2014; published 29 January 2015)

Inelastic tunneling spectroscopy of Pb islands on Cu(111) obtained by scanning tunneling microscopy below 1 K provides a direct access to the local Eliashberg function of the islands with high energy resolution. The Eliashberg function describes the electron-phonon interaction causing conventional superconductivity. The measured Eliashberg function strongly depends on the local thickness of the Pb nanostructures and shows a sharp maximum when quantum well states of the Pb islands come close to the Fermi energy. *Ab initio* calculations reveal that this is related to enhanced electron-phonon coupling at these thicknesses.

DOI: 10.1103/PhysRevLett.114.047002

PACS numbers: 74.81.Bd, 74.25.Jb, 74.25.Kc, 74.50.+r

In conventional superconductors (SCs) Cooper pairs are formed due to electron-electron interaction via virtual phonon exchange. While this concept already lies at the heart of the BCS theory [1], it turned out soon that the simplifications by the assumptions of the BCS theory are too crude. Especially in the strong coupling regime an extension of the theory is required, which was presented by Eliashberg [2]. He took into account that the electron-phonon interaction is local in space and retarded in time. A central quantity in this theory is the effective electron-phonon spectrum  $\alpha^2 F(\omega)$ , which is also called Eliashberg function. Here  $F(\omega)$  is the phonon density of states (DOS) and  $\alpha$  [which actually is  $\alpha(\omega)$ ], is the energy dependent electron-phonon coupling strength. The Eliashberg theory allows us to calculate the properties for all conventional SCs once  $\alpha^2 F(\omega)$  is known.

While the experimental determination of  $F(\omega)$  can be achieved by inelastic neutron scattering, this technique provides no immediate access to the full Eliashberg function since it contains the electron-phonon coupling strength, which is not directly accessible with neutrons. An elegant way to determine the Eliashberg function is to measure the deviation from the BCS density of states of the quasiparticles of a SC extracted from elastic tunneling experiments. It however involves an inversion of the Eliashberg gap equations [3]. Although this method could confirm the validity of the Eliashberg theory it is a rather indirect way of obtaining  $\alpha^2 F(\omega)$ . Especially in the case of multiple superconducting gaps, the inversion is not unique.

Inelastic tunneling spectroscopy (ITS) provides a third and direct access to vibronic excitations in a solid. It has also been used in planar tunneling junctions with Pb films in the normal state to determine the electron-phonon coupling [4]. Using scanning tunneling microscopy

(STM), in addition, offers the possibility of performing ITS with high spatial resolution [5]. Most STM-ITS experiments were dedicated to molecular vibrations but there are, though rarely, studies of collective vibrations as well [6]. The principle of ITS is based on the opening of an inelastic tunneling channel in parallel to the elastic one as soon as the energy of the tunneling electrons overcomes the threshold for inelastic excitation leading to an increase of the differential conductivity  $dI/dU$ . Since the latter is only of a few percent it is common to use a lock-in amplifier and record the second derivative of the tunneling current with respect to the bias voltage,  $d^2I/dU^2$ , which reveals a peak at the positive voltage corresponding to the energy of the excitation. Due to the symmetry of electron and hole tunneling, a minimum (dip) is found at the same voltage on the negative bias side. A dip-peak pair is thus a characteristic fingerprint of an inelastic tunneling process. So far, we only considered excitations at discrete energies. In systems possessing a continuous spectrum of excitations, as in the case of phonons, the second derivative of the tunneling current is proportional to their DOS  $F(\omega)$ :

$$\left. \frac{d^2I}{dU^2} \right|_{U=\hbar\omega/e} \propto \rho_t(E_F)\rho_s(E_F)F(\omega)|M_{\text{inel}}(eU)|^2. \quad (1)$$

Here,  $\rho_t(E_F)$  and  $\rho_s(E_F)$  are the electronic DOSs of the tip and the sample, respectively, and are taken to be constant around  $E_F$ .  $M_{\text{inel}}(eU)$  is the matrix element for inelastic tunneling, which, in the case of phonons, is proportional to the electron-phonon coupling strength  $\alpha$  due to the optical theorem [7]. In a SC, however, the formation of the gap below the superconducting transition temperature  $T_c$  leads to a strong energy dependence of  $\rho_s(E)$  (quasiparticle peaks), which dominate the signal in  $d^2I/dU^2$ . For this

reason, superconductivity has to be suppressed for ITS [4]. In principle, there are two possibilities to force a SC into its normal state even below  $T_c$ . One is to apply a magnetic field, the other one is to use the proximity effect of a SC in contact with a normal metal.

In this Letter, we report on the first direct and spatially resolve the Eliashberg function with STM. We used Pb islands on Cu(111) as a model system for this approach and find strong dependencies of the Eliashberg function on the local electronic properties.

Pb belongs to the so-called strong coupling SCs. The value of  $2\Delta_0/k_B T_c = 4.4$  lies far above the BCS value of 3.53, and it is the material with the strongest electron-phonon coupling among the elemental SCs [8] and has therefore been widely studied in the past. Pb was among the systems that were investigated in the pioneering work of Giaever *et al.* who were able to obtain the quasiparticle DOS from planar tunnel junctions [9]. Indeed, it was this measurement from which the Eliashberg function of a SC was obtained for the first time using the McMillan gap inversion method [3]. The Eliashberg function of Pb exhibits two prominent maxima at around 4 and 8 meV. By regarding the phonon dispersion relation these features can be ascribed to van Hove singularities of the transverse and longitudinal phonon modes, respectively [10–12].

In recent years, especially thin Pb islands attracted much attention since the vertical confinement of the electrons results in discrete quantum well states (QWSs), which were found to have a substantial influence on the growth mode [13–15]. When Pb is deposited onto Cu(111) at room temperature (RT), the growth mode is of Stranski-Krastanov type [16]; i.e., islands start to grow once a wetting layer (WL) is complete. These islands are (111)-oriented nanocrystallites with a height distribution that is not statistical. Instead, as was first observed by Budde *et al.*, certain “magic” heights are strongly preferred while some other numbers of monolayers (MLs) seem to be “forbidden” [13,17]. Otero *et al.* showed that the appearance of these preferred heights is directly correlated to the QWSs. A thickness for which a QWS is near the Fermi level is energetically unfavored and thus, when growing, the system avoids those numbers of MLs. Moreover, an influence of the QWSs on the electron-phonon coupling and on  $T_c$  has been demonstrated for Pb films on semiconducting Si(111). Different results were published, in which  $T_c$  rises [18–20] or slightly falls [21] with increasing film thickness superimposed with weak oscillations. In contrast, Pb islands on Cu(111) are expected to be in the normal state due to the proximity effect of the metallic substrate [22]. Hence, Pb/Cu(111) should provide an ideal system to study the phonon excitations by STM-ITS in the normal state and to resolve the details of the influence of the QWSs on the Eliashberg function as well.

The preparation and study of the samples were carried out in UHV in a homemade low temperature STM setup

[23]. In particular, it comprises a Joule-Thomson refrigerator operated with a  $^3\text{He}$ - $^4\text{He}$  mixture, which allows for a base temperature below 700 mK. The Cu substrates and the lead films were free from impurities on the detection level of STM. The Cu(111) single crystal was cleaned by  $\text{Ar}^+$  sputtering and subsequent annealing. After the sample had cooled down to RT, Pb was deposited. A W tip, which was treated by several cycles of  $\text{Ar}^+$  sputtering and flash annealing, was used. The temperature of the sample and the tip was  $(0.8 \pm 0.1)$  K during the measurements. For ITS the tip was stabilized at 20 mV and 50 nA (i.e.,  $R_T = 0.4$  M $\Omega$ ) and the spectra were obtained by measuring the second derivative of the tunneling current using the lock-in technique with a modulation voltage of 400  $\mu\text{V}$  (rms) at 16.2 kHz resulting in an energy resolution  $\Gamma$  of 0.78 meV [5]. The acquisition time for one spectrum was about 1 h in order to achieve a sufficient signal-to-noise ratio.

Figure 1(a) shows a typical STM topography of a sample after depositing a total amount of 3.8 MLs. Pb islands of a lateral size of about 100 nm grow on top of the wetting layer on the stepped Cu(111) surface. Most of the islands span one or more Cu steps and many of them coalesce. In order to determine the local thickness we considered the height profiles extracted from the STM topography as well as the QWSs [17]. In Fig. 1(a) the Pb areas are marked with different colors according to their local thickness whereas Fig. 1(b) shows the thickness distribution. Most of the

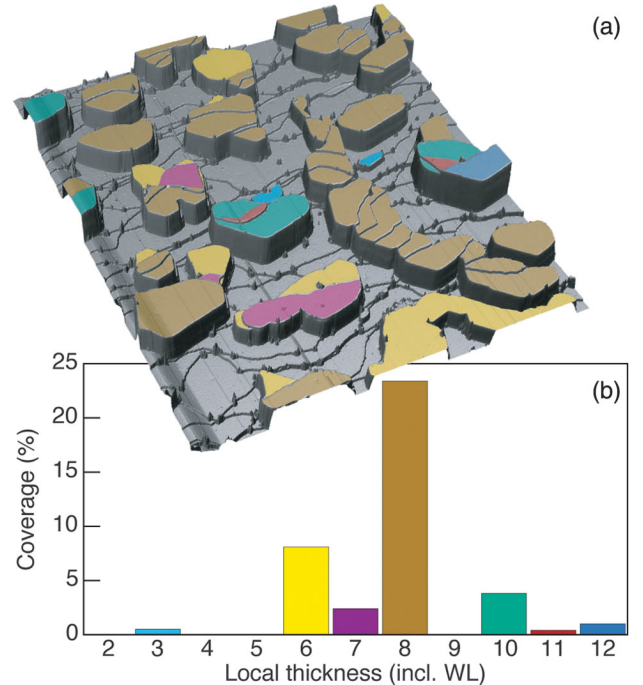


FIG. 1 (color). (a) STM topography ( $800 \times 800$  nm $^2$ , 1 V, 100 pA) showing Pb islands on the stepped Cu(111) surface after depositing a total amount of 3.8 MLs. The colored surfaces indicate the local thickness whose distribution is given in (b).

islands have a constant thickness of six or eight MLs including the wetting layer, which are thus the “magic heights” for this amount of Pb. As can be seen in Figs. 1(a) and 3(a), there are, however, some islands that change their thickness by one or two MLs when growing over a Cu step edge and closely spaced steps may even help to stabilize unfavored heights, as was already observed before [17]. In particular, there are only two rather small regions in Fig. 1(a) that are 11 MLs thick and 9 MLs were not observed at all. Another sample with a nominal coverage of 16 MLs provided access to Pb slabs of 17 to 33 MLs (not shown).

We performed  $dI/dU$  spectroscopy on the Pb regions of different heights as well as on the wetting layer. In Fig. 2 we show exemplarily the results for a Pb thickness of 13 MLs. In contrast to the constant differential conductance of the WL there is a pronounced dip around  $E_F$  in the case of the 13 MLs Pb island. The same effect was observed for Pb islands of various thickness on Si(111) [24]. Since that experiment was performed at 10 K, which is above  $T_c$  of Pb, the authors termed this feature a “pseudogap.” Further, they report on “pseudo-peaks” in the case of 18 MLs and 27 MLs. In contrast, for Pb on Cu(111) we did not observe peaks at these thicknesses but only dips of different intensity. The phenomenological model of Wang *et al.*, borrowed from optics, thus does not apply to Pb on

Cu(111). By attributing the dip to inelastic excitations we give an alternative explanation in the case of Pb on Cu(111). Figure 2(b) presents a high resolution  $d^2I/dU^2$  spectrum of the relevant energy range. An almost point-symmetric shape is obtained showing two dominant dip-peak pairs at a bias of about  $\pm 4.0$  and  $\pm 8.5$  mV as well as one very close to zero bias ( $\pm 0.6$  mV). A comparison to the previously determined Eliashberg function of Pb [3] is provided in Fig. 2(c) and since it reveals an almost perfect agreement there is strong evidence that the ITS data directly yield the Eliashberg function, i.e., the dip does not indicate a pseudogap. Only the feature closest to  $E_F$  is not related to  $\alpha^2F(\omega)$  but is due to a zero bias anomaly, as already observed in planar tunneling experiments on Pb [25].

After confirming that STM-ITS is able to measure the Eliashberg function we focused on the thickness dependence. In particular, we investigated a “wedge”-like island [Fig. 3(a)], the height of which increases by 1 ML at every underlying step starting from 11 MLs. Keeping all parameters constant, we recorded  $d^2I/dU^2$  spectra [Fig. 3(d)] on

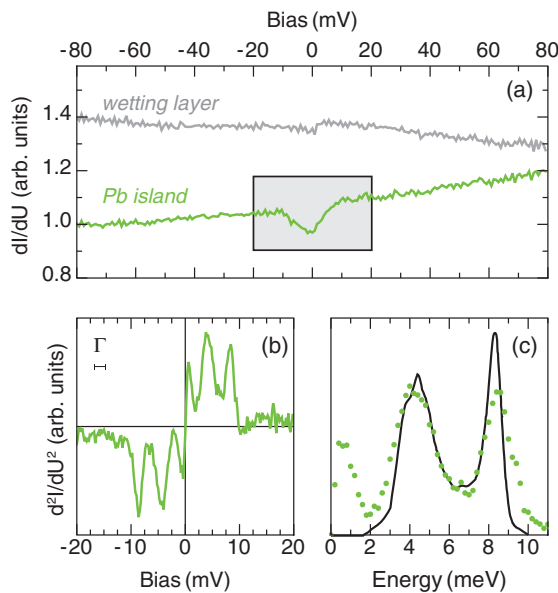


FIG. 2 (color). (a) Large energy range tunneling conductance spectra (normalized and shifted) of the WL and of a 13 MLs Pb area ( $R_T = 8 \text{ M}\Omega$ ). While the conductance of the WL is constant, it exhibits a significant decrease at zero bias on the Pb island, it exhibits a significant decrease at zero bias on the Pb island.  $d^2I/dU^2$  spectrum (b) taken on the same position in a smaller bias interval around  $E_F$  ( $R_T = 0.4 \text{ M}\Omega$ ). The scale bar indicates the energy resolution  $\Gamma$ . (c) Average of the positive and negative bias side of the ITS spectrum in (b) (dots) in comparison with the previous result for  $\alpha^2F(\omega)$  (line) [3].

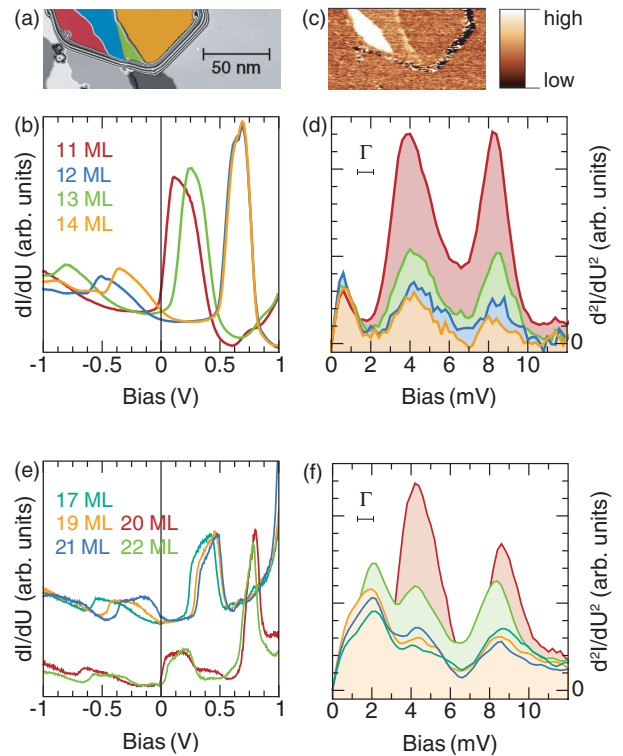


FIG. 3 (color). (a) Topographic image of a wedge shaped island. The color code of the Pb areas corresponds to the thicknesses given in (b) where the QWSs obtained from the  $dI/dU$  spectra ( $R_T = 0.1 \text{ G}\Omega$ ) at an arbitrary location on the Pb areas of different heights are shown. (d) Average of the positive and negative bias side of the  $d^2I/dU^2$  spectra ( $R_T = 0.4 \text{ M}\Omega$ ) recorded at the same locations as in (b). The intensity of  $\alpha^2F(\omega)$  increases considerably on the 11 MLs high Pb area as can also be seen from the  $d^2I/dU^2$  map of the same island taken at 8 mV (c). QWSs (e), and  $d^2I/dU^2$  spectra (f) of 17 to 22 MLs.

every local thickness and we were able to find the zero bias anomaly and the Eliashberg function in all cases. While the former stays the same there is a strong thickness dependence of the intensity of  $\alpha^2F(\omega)$ . Note that the energies of the phonon peaks stayed constant indicating a thickness independent phonon spectrum in the studied thickness range as previously predicted [26]. For areas comprising 12 and 14 MLs it is relatively weak whereas the signal gets stronger for 13 MLs and is by far strongest for 11 MLs as can also be seen in the  $d^2I/dU^2$  map, i.e., a map of the local electron-phonon coupling at 8 meV, in Fig. 3(c) recorded with the bias set to the energy of the longitudinal peak. No differences were found for different locations within an area of a given thickness confirming the absence of impurity scattering in the lead film. Note that in all experiments, the current was set to the same value during tip stabilization, such that the differences in the inelastic spectra are not related to differences in the electronic DOS. Since we expected that the thickness dependence should be influenced by the electronic QWSs, we measured the first derivative of the tunneling current in a larger voltage range [Fig. 3(b)]. For 12 and 14 MLs, the highest occupied as well as the lowest unoccupied states lie roughly 0.5 eV away from the Fermi level. In contrast, the lowest unoccupied QWSs of the 11 and 13 MLs thick layers are very close to  $E_F$ . The relevant QWS of the former, which exhibited also the highest  $\alpha^2F(\omega)$  intensity, is closest to  $E_F$ . Thus, our experiment clearly shows, that electron-phonon coupling can be strongly enhanced (factor of 5), if unoccupied QWSs are near the Fermi energy. Figures 3(e) and 3(f) reveal the same effect for thicker Pb slabs on the other sample.

To elucidate the experimental finding, we calculated the electronic structure and phonons for different Pb films on Cu(111). The structural relaxations and the phonons were computed using the VASP code, well known for precise total energy and forces calculations [27], while the electronic structure of the thin films was obtained with a first-principles Green's function method, specially designed for semi-infinite systems such as surfaces and interfaces [28]. The self-consistently calculated Green's functions and phonons were used to compute the Eliashberg function of the given systems.

First of all, we found QWSs in these systems in qualitative agreement with the experiment. The calculated electronic DOS exhibits a QWS closest to the Fermi level for a thickness of 11 MLs and a little further for 13 MLs while for 12 MLs and 14 MLs the highest occupied and the lowest unoccupied QWSs are located almost symmetrically around  $E_F$  [Fig. 4(a)]. The theoretical results for  $\alpha^2F(\omega)$  in Fig. 4(b) reveal the same effect as the experiment. While the intensity of  $\alpha^2F(\omega)$  is the same for 12 and 14 MLs, it increases by more than 30% in the case of 13 MLs. For the 11 MLs slab the QWS is even closer to  $E_F$ , which again is accompanied by a further increase of the intensity of

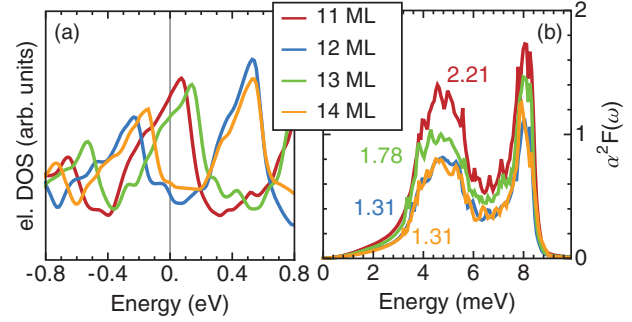


FIG. 4 (color). Theoretical calculation. (a) QWS in the electronic DOS. (b) Eliashberg function. The numbers indicate the corresponding values of  $\lambda$ .

$\alpha^2F(\omega)$ . The resulting electron-phonon coupling constant  $\lambda$ , which changes from a value of about 1.3 to 2.2, i.e., significantly above the bulk value, upon the shift of the QWS towards  $E_F$  is indicated in the figure. Thus, in qualitative agreement to the experiment, the Eliashberg function can be increased by an unoccupied QWS near the Fermi level. Quantitatively, the experimental enhancement of the electron-phonon coupling is even stronger than theoretically predicted by a factor of 2–3, possibly due to the details of the quantum well states of Pb on Cu(111). Similarly, Brun *et al.* showed in their *ab initio* calculations of freestanding Pb films between 4 and 10 MLs an influence of the DOS at  $E_F$  on  $\lambda$ . In their calculations an enhanced  $\lambda$  was observed especially for five MLs, while for thicker films, the bulk value is approached. We speculate that this difference is due to the freestanding nature of the calculated films, which prevent a precise energetic alignment of the QWS with respect to the Fermi level.

The mechanism leading to the enhancement can be understood from total energy considerations. The formation of QWSs in thin Pb films leads to an energetically unfavorable condition when a QWS lies very close to  $E_F$ . A change of the lattice constant, e.g., by a phonon, shifts the QWS up and down through the Fermi level, thus maximizing electron-phonon scattering near the Fermi edge. This enhanced electron-phonon scattering enters the Eliashberg function and is thus detectable by ITS. Further, this effect should influence  $T_c$ . Supposing that the behavior is similar on Si(111), our findings could also explain the  $T_c$  oscillation with thickness as it was observed in that system [21].

In conclusion, we demonstrated that, using low temperature STM-ITS, it is possible to directly measure phonon excitations in Pb islands. The obtained  $d^2I/dU^2$  spectra can be unambiguously identified as  $\alpha^2F(\omega)$ , which allows for the experimental determination of the latter with the high spatial resolution of STM. We found a pronounced dependence of the Eliashberg function on the thickness of the Pb slabs, which, with the aid of *ab initio* calculations,

can be explained by their energetic stability due to the position of the electronic QWSs. This mechanism, if generally applicable, can be used to increase  $T_c$  of conventional superconductors by using layered structures with QWSs at appropriate energies.

M. S. acknowledges funding by the Karlsruhe House of Young Scientists (KHYS).

- 
- [1] J. Bardeen, L. N. Cooper, and J. R. Schrieffer, *Phys. Rev.* **108**, 1175 (1957).
- [2] G. M. Eliashberg, *J. Exptl. Theoret. Phys. (U.S.S.R.)* **38**, 966 (1960).
- [3] W. L. McMillan and J. M. Rowell, *Phys. Rev. Lett.* **14**, 108 (1965).
- [4] J. M. Rowell, W. L. McMillan, and W. L. Feldmann, *Phys. Rev.* **180**, 658 (1969).
- [5] B. C. Stipe, M. A. Rezaei, and W. Ho, *Science* **280**, 1732 (1998).
- [6] L. Vitali, M. A. Schneider, K. Kern, L. Wirtz, and A. Rubio, *Phys. Rev. B* **69**, 121414 (2004).
- [7] C. Cohen-Tannoudji, F. Diu, and F. Laloë, *Quantenmechanik 2* (de Gruyter, Berlin 2010).
- [8] W. Buckel, *Supraleitung: Grundlagen und Anwendungen* (Wiley, New York, 2004).
- [9] I. Giaever, H. R. Hart, and K. Megerle, *Phys. Rev.* **126**, 941 (1962).
- [10] R. Heid, K.-P. Bohnen, I. Y. Sklyadneva, and E. V. Chulkov, *Phys. Rev. B* **81**, 174527 (2010).
- [11] B. N. Brockhouse, T. Arase, G. Caglioti, K. R. Rao, and A. D. B. Woods, *Phys. Rev.* **128**, 1099 (1962).
- [12] R. Stedman, L. Almqvist, and G. Nilsson, *Phys. Rev.* **162**, 549 (1967).
- [13] K. Budde, E. Abram, V. Yeh, and M. C. Tringides, *Phys. Rev. B* **61**, R10602 (2000).
- [14] R. Otero, A. L. Vázquez de Parga, and R. Miranda, *Surf. Sci.* **447**, 143 (2000).
- [15] W. B. Su, S. H. Chang, W. B. Jian, C. S. Chang, L. J. Chen, and T. T. Tsong, *Phys. Rev. Lett.* **86**, 5116 (2001).
- [16] J. Camarero, J. Ferrón, V. Cros, L. Gómez, A. L. Vázquez de Parga, J. M. Gallego, J. E. Prieto, J. J. de Miguel, and R. Miranda, *Phys. Rev. Lett.* **81**, 850 (1998).
- [17] R. Otero, A. L. Vázquez de Parga, and R. Miranda, *Phys. Rev. B* **66**, 115401 (2002).
- [18] Y.-F. Zhang, J.-F. Jia, T.-Z. Han, Z. Tang, Q.-T. Shen, Y. Guo, Z. Q. Qiu, and Q.-K. Xue, *Phys. Rev. Lett.* **95**, 096802 (2005).
- [19] Y. Guo, Y.-F. Zhang, X.-Y. Bao, T.-Z. Han, Z. Tang, L.-X. Zhang, W.-G. Zhu, E. G. Wang, Q. Niu, Z. Q. Qiu *et al.*, *Science* **306**, 1915 (2004).
- [20] C. Brun, I.-Po Hong, F. Patthey, I. Yu. Sklyadneva, R. Heid, P. M. Echenique, K. P. Bohnen, E. V. Chulkov, and W.-D. Schneider, *Phys. Rev. Lett.* **102**, 207002 (2009).
- [21] D. Eom, S. Qin, M.-Y. Chou, and C. K. Shih, *Phys. Rev. Lett.* **96**, 027005 (2006).
- [22] P. Hilsch, *Z. Phys.* **167**, 511 (1962).
- [23] L. Zhang, T. Miyamachi, T. Tomanić, R. Dehm, and W. Wulfhekel, *Rev. Sci. Instrum.* **82**, 103702 (2011).
- [24] K. Wang, X. Zhang, M. M. T. Loy, T.-C. Chiang, and X. Xiao, *Phys. Rev. Lett.* **102**, 076801 (2009).
- [25] W. J. Wattamaniuk, H. J. Kreuzer, and J. G. Adler, *Phys. Lett.* **37A**, 7 (1971).
- [26] M. Jalochowski, *Z. Phys. B* **56**, 21 (1984).
- [27] G. Kresse and J. Furthmüller, *Phys. Rev. B* **54**, 11169 (1996).
- [28] M. Lüders, A. Ernst, W. M. Temmerman, Z. Szotek, and P. J. Durham, *J. Phys. Condens. Matter* **13**, 8587 (2001).